

Saturation of nuclear matter in effective field theory

P. Saviankou¹, S. Krewald¹, E. Epelbaum^{1,2}, and Ulf-G. Meißner^{2,1}

¹ Institut für Kernphysik, Forschungszentrum Jülich, D-52425 Jülich, Germany

² Universität Bonn, Helmholtz-Institut für Strahlen- und Kernphysik, Nußallee 14-16, D-53115 Bonn, Germany

Received: date / Revised version: date

Abstract. The two-nucleon interaction derived in chiral effective field theory is used to investigate the saturation properties of symmetric nuclear matter at next-to-leading order. Pauli blocking effects in the two-pion exchange diagrams are shown to produce an effective attraction in nuclear matter.

PACS. 21.65.-f Nuclear matter – 21.65.Mn Equation of state of nuclear matter – 21.30.-x Forces in hadronic systems

Within the last two decades, effective field theory has provided new methods for nuclear structure investigations. Two-, three- and four-nucleon interactions based on the most general chiral effective pion-nucleon Lagrangian have been developed based on Weinberg's power counting scheme. The phase shifts of the nucleon-nucleon interaction below the pion production threshold are reproduced with a precision that is comparable with the one achieved by modern phenomenological two-nucleon potentials, when pushing the expansion to the order $N^3\text{LO}$,¹ see Refs.[1,2]. These forces together with three-nucleon forces at $N^2\text{LO}$ have been applied to a cornucopia of reactions. In particular, various three-nucleon scattering observables have been analyzed at low and intermediate energies showing, in general, a good agreement with the data. The binding energies of ^3He and ^4He have been reproduced successfully once the leading three-nucleon force is included. Within the framework of the no-core shell model, the chiral forces have been used to study nuclei with $A = 7, 10 \dots 13$ systems, in particular the sensitivity to the three-nucleon force, see [3,4] for more details. Recent progress in these fields is reviewed in Ref. [5]. Given these successes, the question arises whether effective field theory can contribute to the solution of the nuclear matter problem. First ground-breaking attempts in this direction have been done by the Munich group, see e.g. Refs. [6,7] (and references therein). In the present communication, we apply the NLO version of the chiral nucleon-nucleon interaction to symmetric nuclear matter. This differs from the Munich approach which concentrates on the development of a chiral effective interaction to be used exclusively in the nuclear medium without link to the two-nucleon interaction in the vacuum. In Ref.[8], nuclear matter has been studied with a low-momentum two-nucleon force $V_{\text{low-k}}$ derived from the Ar-

gonne v_{18} potential via renormalization group techniques. It was found that the low-momentum interactions can be used in second order perturbation theory to describe nuclear matter, provided Pauli blocking effects due to the medium are properly included. This finding suggests that a resummation of the ladder diagrams, as it is mandatory in Brueckner theory, can be avoided. Recently, the simplified version $AV6'$ of the Argonne potential has been used in a quantum Monte Carlo study of symmetric nuclear matter [9]. For Fermi momenta less than $k_F = 1.33 \text{ fm}^{-3}$, the binding energies obtained for nuclear matter are not smaller than the ones calculated within the Fermi hypernetted chain approach or the Brueckner Hartree-Fock method [10]. This fact is interpreted as evidence for the inadequacy of three-nucleon interaction models for all densities [9].

Both the two-nucleon potential derived from effective field theory and $V_{\text{low-k}}$ derived from any of the high-precision NN potentials can be characterized by the fact that the large momentum components of the interaction are removed, in contrast to meson-exchange potentials.

The chiral potential differs from phenomenological ones, such as v_{18} , by its power counting scheme which allows systematic improvements. In Ref.[13], the pion-nucleon vertices are systematically taken from the chiral expansion of the pion-nucleon interaction. The two-nucleon interaction is generated by eliminating the pion-two-nucleon states via the FST-Okubo projection method [11,12]. The two-pion exchange diagrams relevant for the discussion of nuclear matter properties are shown in Fig.1 for the order NLO. The Weinberg-Tomozawa term generates a class of triangle diagrams (c) characterized by one internal nucleon line. Moreover, there are diagrams with two internal nucleon lines, such as the crossed-box two-pion exchange graph (a). Notice that the class of box two-pion exchange diagrams (b) in Fig.1 is not two-nucleon reducible and therefore has to be iterated when solving the Schrödinger

¹ Throughout, we use the abbreviation LO for leading order, NLO for next-to-leading order and so on.

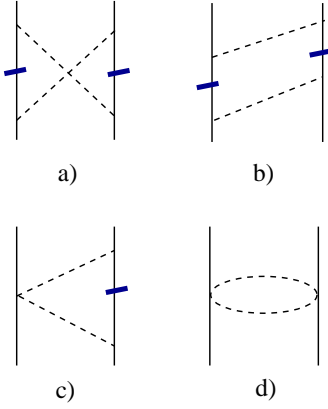


Fig. 1. Two-pion exchange corrections to the chiral two-nucleon potential in NLO. a) crossed box graph, b) wave function renormalization diagram, c) Triangle graph, and d) football diagram. Solid/dashed lines denote nucleons/pions. The thick lines indicate medium modifications due to Pauli blocking.

equation for two-nucleon scattering [14]. Also present are the so-called football diagrams (d), however, these do not have internal in-medium nucleon propagators. In the nuclear medium, the two-nucleon interaction evaluated in the vacuum is strongly modified by Pauli blocking effects. The most important and well-known Pauli blocking effect affects the intermediate two-nucleon states. For the chiral two-nucleon interaction, there are additional Pauli blocking effects due to the intermediate one- and two-nucleon propagators in the diagrams shown in Fig.1. Formally, these Pauli blocking effects can easily be taken into account. The chiral potential is derived in Ref. [14] using the FST-Okubo method of unitary transformations, introducing a projector η on the two-nucleon space and a projector λ for the remaining part of the Fock space which consists of two-nucleon and one-pion or multi-pion states. The corresponding unitary operator is parametrized in terms of the transition operator $A = \lambda A \eta$ which fulfills the decoupling equation

$$\lambda(H - [A, H] - AHA)\eta = 0. \quad (1)$$

This equation is solved perturbatively utilizing the chiral power counting. Once A is computed at a given order in the chiral expansion, the effective Hamilton operator acting on the nucleonic subspace of the Fock space can be obtained in a straightforward way. In the nuclear medium, one has to introduce medium-modified projectors

$$\bar{\eta} = \int d^3 k_1 \int d^3 k_2 (1 - \Theta(\mathbf{k}_1))(1 - \Theta(\mathbf{k}_2)) \times |\mathbf{k}_1 \mathbf{k}_2\rangle \langle \mathbf{k}_1 \mathbf{k}_2|, \quad (2)$$

$$\bar{\lambda} = \int d^3 k_1 \int d^3 k_2 \int d^3 q_\pi (1 - \Theta(\mathbf{k}_1))(1 - \Theta(\mathbf{k}_2)) \times |\mathbf{k}_1 \mathbf{k}_2 q_\pi\rangle \langle \mathbf{k}_1 \mathbf{k}_2 q_\pi| + \dots, \quad (3)$$

ellipses refer to components with two and more pions, $\Theta(\mathbf{k}) = 1$ for $k \leq k_F$ and $\Theta(\mathbf{k}) = 0$ for $k > k_F$. The

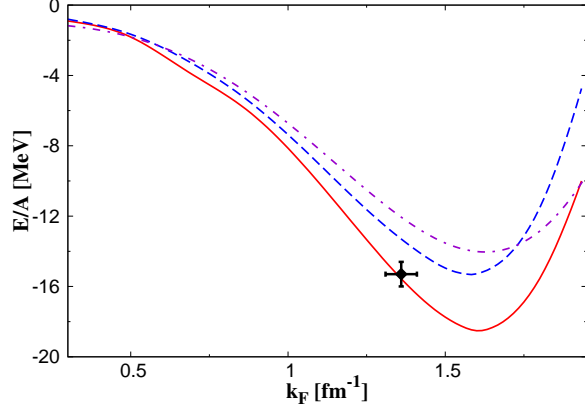


Fig. 2. The binding energy per particle of nuclear matter as a function of the Fermi momentum k_F . Solid (red) line: The Pauli blocking effects due to Eqs. (2,3) are included. Dashed (blue) line: Pauli blocking effects of Fig. 1 not included. Dash-dotted (violet) line: AFDMC results [9]. The empirical saturation point is given by the black circle.

momenta of the two nucleons and the pion are denoted by $\mathbf{k}_1, \mathbf{k}_2$ and \mathbf{q}_π , respectively. The diagrams shown in Fig.1 require loop integrations over non-trivial integration volumes defined by the Pauli blocking constraints. The binding energy is obtained by summing all two-nucleon reducible diagrams, as it is done in Brueckner-Hartree-Fock theory. Therefore, the perturbative calculation of Ref.[8] can be considered as the limit of the present approach for weak potentials. At NLO, genuine three-body forces are not yet included.² The two-nucleon interactions derived in Ref. [2] are characterized by two regulators, the cut-off $\tilde{\Lambda}$ introduced in the spectral function representation of the two-pion exchange diagrams and the cut-off Λ required for the non-perturbative renormalization of the Lippmann-Schwinger equation. The actual potentials are derived for a large set of regulators $\tilde{\Lambda}$ and Λ in order to generate theoretical error bands for a given order of the expansion. Nuclear matter introduces a new scale into effective field theory, the Fermi momentum, empirically given by $k_F = 262$ MeV. The effective two-nucleon interaction in nuclear matter should be able to describe momentum transfers of about $2k_F$. Therefore we have restricted the nuclear matter calculations to those potentials which have Lippman-Schwinger regulators $\Lambda \geq 500$ MeV. Fig. 2 shows the binding energy per particle as a function of the Fermi momentum k_F for the NLO potential of Ref. [2] derived for $\Lambda = 550$ MeV and $\tilde{\Lambda} = 500$ MeV. densities. One finds that at NLO, the chiral two-nucleon interaction produces a saturation point for nuclear matter, though not at the empirical values for the density and binding energy.

In Refs. [8], the three-body forces were found to be essential in order to obtain saturation in a perturbative scheme. In the chiral approach of Ref. [7], the effect of three-body forces has been studied in detail. The calcu-

² A rough estimate of the effect of three-nucleon forces has been given in Ref. [16].

lation including three-body forces saturates at the empirical density of nuclear matter $\rho_{exp} = 0.160 \text{ fm}^{-3}$, if a pion-nucleon form factor of monopole type is used with a cut off $\Lambda_0 = 1145 \text{ MeV}$. A calculation without three-body forces can obtain saturation at ρ_{exp} , provided the cut off is reduced to $\Lambda_0 = 770 \text{ MeV}$. The saturation found in the present calculation is entirely due to the regulators because there are no three-body forces at NLO. At order N^2LO , chiral three-body forces appear which will reduce the sensitivity of the results to the choice of the regulators.

The present calculation provides quantitative results concerning the relevance of the Pauli corrections imposed by Eqs. (2,3). We parameterize the saturation curves following Ref. [9] by

$$\frac{E}{A} = \frac{E_0}{A} + \alpha(x - \bar{x})^2 + \beta(x - \bar{x})^3, \quad (4)$$

with $x = \rho/\rho_{exp}$ and $\rho_{exp} = 0.160 \text{ fm}^{-3}$ and obtain a binding energy $E_0/A = -18.35 \text{ MeV}$ at a Fermi momentum $k_F = 1.60 \text{ fm}^{-1}$ for the calculation which includes the Pauli blocking effects due to Eqs. (2,3). The compression modulus of nuclear matter then is given by $K = 279 \text{ MeV}$, corresponding to $\alpha = 5.0 \text{ MeV}$ and $\beta = -0.34 \text{ MeV}$. This is slightly larger than the value of the compression modulus derived from giant resonances, $K = (260 \pm 10) \text{ MeV}$ [17]. A discussion of the model dependence of the compression modulus can be found in Ref.[18]. If one discards the Pauli blocking effects due to Eq.(3), the saturation point moves to $E_0/A = -15.30 \text{ MeV}$ and $k_F = 1.57 \text{ fm}^{-1}$, and a compression modulus of $K = 244 \text{ MeV}$ is obtained. In order to understand the medium effects due to Eqs. (2,3), we have studied the influence of the various classes of the bare two-nucleon interactions on the two-nucleon phase shifts by multiplying the contributions of individual diagrams with some numerical factor. For the most important 3S_1 and 1S_0 phase shifts, the (numerically) dominant contribution arises from diagrams a) in Fig.1 and is repulsive in both cases. In nuclear matter, the Pauli blocking of the diagrams involving two pion lines effectively reduces the repulsive contribution to the two-nucleon potential. Therefore, a gain of binding energy results, as seen in the calculations shown in Fig. 2. Quantitatively, the gain of binding energy is large enough to pull the saturation curve below the empirical saturation point of nuclear matter. The overall gain of binding energy in the vicinity of the saturation density is about 3 MeV. Genuine three-body interactions tend to yield an overall repulsive contribution to the binding energy. The new class of Pauli blocking effects studied in the present work may therefore be helpful to move the theoretical saturation point closer to the empirical value. Ref.[2] shows error bands for each phase shift which reflect the theoretical uncertainty due to the choice of the regulators. In Fig. 3 we show the corresponding uncertainties for the nuclear matter saturation curve limiting ourselves to the variation of the cut-off Λ . The calculations have been performed omitting the Pauli blocking effects due to Eqs. (2,3) because the full inclusion of those effects is numerically time-consuming. This simplified calculation, however, already provides a reason-

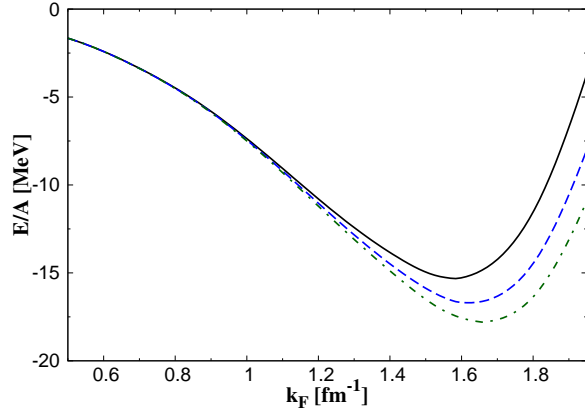


Fig. 3. Dependence on the spectral function cut-off of the saturation curve. The Pauli blocking effects due to Eqs. (2) are included. The solid (black), dashed (blue) and dash-dotted (green) line refer to the spectral function cut-offs $\Lambda = 500, 600$ and 700 MeV , respectively.

able estimation of the theoretical uncertainty. In the limit of low densities one observes that the binding energies do not depend on the regulator employed. A similar observation can be found in Ref.[7]. It may be understood as an illustration of Hugenholtz's well-known justification of Brueckner's method to describe the energy of a Fermi gas in the low density limit by summing the ladder diagrams of the two-body interactions[15]. At NLO, the saturation points are clearly cut-off dependent. The Fermi momentum at the saturation point varies from $k_F = 1.59 \text{ fm}^{-1}$ to $k_F = 1.66 \text{ fm}^{-1}$, while the binding energy per particle moves from -15.3 MeV to -17.8 MeV .

One of the most successful effective interactions to be used for the description of nuclear ground states has been proposed by Skyrme, see Ref.[18] for a recent review. In its simplest version, this interaction introduces contact interactions which have an analytical structure similar to the contact terms of the chiral two-nucleon potential. The Skyrme interaction differs from chiral interactions by introducing a contact three-body term

$$v(\mathbf{r}_1, \mathbf{r}_2, \mathbf{r}_3) = t_3 \delta(\mathbf{r}_1 - \mathbf{r}_2) \delta(\mathbf{r}_2 - \mathbf{r}_3). \quad (5)$$

A term like this is not produced by the leading chiral three-body interactions[16]. Moreover, if interpreted as a genuine three-body interaction, it leads to well-known spin instabilities[19] in nuclei signalled by the Landau parameter $g_0 = -t_3/8$. In practical calculations, one therefore replaces the three-body interaction by a density-dependent two-body interaction $v = t_3/6\rho^\alpha$ with $\alpha = 1$, effectively freezing the unphysical spin dependence of Skyrme's three-nucleon interaction. For the following comparison, we do not try to interpret the density-dependent term as a genuine three-body interaction, but rather as an effective representation of a regulator. In Ref. [14], an exponential regulator

$$f_n(q, \Lambda) = \exp(-(q/\Lambda)^{2n}) \quad (6)$$

Table 1. Skyrme force parameters. The column NLO list the parameters obtained from fits to the two-nucleon interaction Ref.[2], while the ones resulting from the fits to finite nuclei, Ref.[20], are listed in column Skyrme.

Parameter	NLO	Skyrme
$t_0[\text{MeV fm}^3]$	$-778 \dots -643$	-930
x_0	$0.17 \dots 0.41$	$0.0 \dots 0.40$
$t_1[\text{MeV fm}^5]$	$240 \dots 260$	$77 \dots 130$
$t_2[\text{MeV fm}^5]$	-23	$-80 \dots 0$

for the Lippmann-Schwinger equation has been used. In nuclear matter, the states close to the Fermi surface dominate. Therefore, one can approximate the averaged contributions to the potential energy by replacing the momentum in the regulator by the Fermi momentum and subsequently expanding the regulator, obtaining

$$\overline{f_n(q, A)v(q, q')f_n(q, A)} = \alpha + \beta k_F^{2n}. \quad (7)$$

The term proportional to β can be interpreted as an effective density-dependent interaction of the Skyrme type with a density dependence ρ^α , the power of the density dependence being $\alpha = 2n/3$. A least squares fit to the nuclear ground state energies and radii for a large set of nuclei has been performed in Ref.[20] as a function of the power α of the density dependence. The regulator employed in Ref. [14] is defined by $n = 2$ and corresponds to an exponent $\alpha = 4/3$ of the density dependence of the Skyrme interaction. The corresponding Skyrme parameters t_0, x_0, t_1, t_2 are displayed in Table 1. The chiral two-nucleon interaction has contact terms proportional to C_S and C_T which translate into Skyrme parameters $t_0 = C_S - C_T$ and $x_0 = 2C_S/(C_S - C_T)$. Likewise, t_1 and t_2 can be obtained from the NLO terms C_1 and C_2 . Table 1 shows that the Skyrme parameters obtained from the two-nucleon interaction at order NLO agree in relative sign and are of the same order of magnitude as the ones deduced by fitting directly the bulk properties of finite nuclei.

The present study demonstrates the applicability of the chiral two-nucleon interactions to nuclear matter and justifies the efforts required to investigate the next-to-next-to-leading order.

A helpful comment by Victor Tselyaev is gratefully acknowledged. We thank the DFG for partial support by the grant GZ:432RUS113/806/0-1. This work was further supported in parts by funds provided from the Helmholtz Association to the young investigator group “Few-Nucleon Systems in Chiral Effective Field Theory” (grant VH-NG-222) and the Virtual Institute “Spin and strong QCD” (grant VH-VI-231). This work was further supported by the DFG (SFB/TR 16 “Subnuclear Structure of Matter”) and by the EU I3HP Project under contract number RII3-CT-2004-506078.

References

1. D. R. Entem and R. Machleidt, Phys. Lett. B **524** (2002) 93 [arXiv:nucl-th/0108057].
2. E. Epelbaum, W. Glöckle and U.-G. Meißner, Nucl. Phys. A **747** (2005) 362 [arXiv:nucl-th/0405048].
3. A. Nogga, P. Navratil, B. R. Barrett and J. P. Vary, Phys. Rev. C **73** (2006) 064002 [arXiv:nucl-th/0511082].
4. P. Navratil, V. G. Gueorguiev, J. P. Vary, W. E. Ormand and A. Nogga, Phys. Rev. Lett. **99** (2007) 042501 [arXiv:nucl-th/0701038].
5. E. Epelbaum, Prog. Part. Nucl. Phys. **57** (2006) 654 [arXiv:nucl-th/0509032].
6. N. Kaiser, S. Fritsch and W. Weise, Nucl. Phys. A **697** (2002) 255 [arXiv:nucl-th/0105057].
7. N. Kaiser, M. Muhlbauer and W. Weise, Eur. Phys. J. A **31** (2007) 53 [arXiv:nucl-th/0610060].
8. S. K. Bogner, A. Schwenk, R. J. Furnstahl and A. Nogga, Nucl. Phys. A **763** (2005) 59 [arXiv:nucl-th/0504043].
9. S. Gandolfi, F. Pederiva, S. Fantoni and K. E. Schmidt, Phys. Rev. Lett. **98** (2007) 102503 [arXiv:nucl-th/0607022].
10. I. Bombaci, A. Fabrocini, A. Polls and I. Vidana, Phys. Lett. B **609** (2005) 232 [arXiv:nucl-th/0411057].
11. N. Fukuda, K. Sawada and M. Taketani, Prog. Theor. Phys. **12** (1954) 156.
12. S. Okubo, Prog. Theor. Phys. **12** (1954) 603.
13. E. Epelbaum, W. Glöckle and U.-G. Meißner, Nucl. Phys. A **637** (1998) 107 [arXiv:nucl-th/9801064].
14. E. Epelbaum, W. Glöckle and U.-G. Meißner, Nucl. Phys. A **671** (2000) 295 [arXiv:nucl-th/9910064].
15. N. M. Hugenholtz, Physica **23** (1957) 533.
16. P. Saviankou, F. Grümmer, E. Epelbaum, S. Krewald, and U.-G. Meißner, Phys. Atom. Nucl. **60** (2006) 1119.
17. D. Vretenar, T. Niksic and P. Ring, Phys. Rev. C **68** (2003) 024310 [arXiv:nucl-th/0302070].
18. J. R. Stone and P. G. Reinhard, Prog. Part. Nucl. Phys. **58** (2007) 587 [arXiv:nucl-th/0607002].
19. B.D. Chang, Phys. Lett. B **60** (1976) 205.
20. J. Friedrich and P. G. Reinhard, Phys. Rev. C **33** (1986) 335.